

Nicorandil and mesenchymal stromal cells attenuate amiodarone-induced liver fibrosis in experimental rats

Heba Mahmoud^{1,2}, Inas Harb^{1,2}, Hala El-hanbuli³, Eman Rashwan^{4,5}, Laila A Rashed⁶, Azza Abusree Ahmed⁶, Abeer Mostafa^{6,*}, 

¹Department of Pharmacology, Faculty of Medicine, Cairo University, Egypt

²Department of Pharmacology, Armed Forces College of Medicine, Cairo, Egypt

³Department of Pathology, Faculty of Medicine, Fayoum University, Fayoum, Egypt

⁴Department of Physiology, Faculty of Medicine, Al-Azhar University, Assuit, Egypt

⁵Department of Physiology, Faculty of Medicine, Jouf University, Sakaka, KSA

⁶Department of Medical Biochemistry and Molecular Biology, Faculty of Medicine, Cairo University, Egypt

Correspondence

Abeer Mostafa, Department of Medical Biochemistry and Molecular Biology, Faculty of Medicine, Cairo University, Egypt

Email: abeer.mostafa@kasralainy.edu.eg; dr_abeer.mostafa@yahoo.com

History

- Received: Oct 25, 2025
- Accepted: Jan 05, 2026
- Published Online: Feb 28, 2026

DOI : [10.15419/w6w5br23](https://doi.org/10.15419/w6w5br23)



Copyright

© Biomedpress. This is an openaccess article distributed under the terms of the Creative Commons Attribution 4.0 International license.



ABSTRACT

Introduction: Hepatic injury is a known side effect of the antiarrhythmic drug amiodarone. The research aimed to assess the possible protective effects of nicorandil and bone marrow-derived mesenchymal stromal cells (MSCs) in amiodarone-induced liver injury. **Methods:** Thirty-six male adult albino rats were divided into the following six groups: 1) normal control; 2) nicorandil group (which received oral nicorandil at 10 mg/kg/day); 3) bone marrow mesenchymal stromal cells (BM-MSCs) group (which received 3×10^6 cells/ml of BM-MSCs suspended in 0.2 ml of phosphate buffered saline (PBS) administered via tail vein injection); 4) amiodarone-induced liver toxicity group (which received oral amiodarone at 25 mg/kg/day once daily); 5) nicorandil-treated group (which received both amiodarone and nicorandil); and 6) MSCs-treated group (which received both amiodarone and BM-MSCs). The fibrotic biomarker transforming growth factor beta-1 (TGF- β 1), as well as the inflammatory biomarkers interleukin-6 (IL-6) and tumor necrosis factor alpha (TNF- α), were assessed by quantitative polymerase chain reaction (qPCR). The oxidative stress markers superoxide dismutase (SOD) and malondialdehyde (MDA) were assessed by enzyme-linked immunosorbent assay (ELISA). Liver function tests, including aspartate transaminase (AST), alanine transaminase (ALT), and albumin, were assessed using colorimetric methods. In support of these analyses, histopathological examination utilizing hematoxylin and eosin (H&E) and Masson's trichrome stains was performed. **Results:** Nicorandil and MSCs efficiently reduced hepatic fibrosis and improved liver function biomarkers. Serum TNF- α , IL-6, TGF- β 1, and MDA values were restored to nearly normal levels. **Conclusion:** Nicorandil and MSCs are promising hepatoprotective agents against amiodarone-induced hepatic toxicity through their antioxidant and anti-inflammatory potentials.

Key words: MSCs, Nicorandil, TNF- α , IL-6, TGF, MDA, SOD

INTRODUCTION

Amiodarone (AMD), a prevalent antiarrhythmic agent, is implicated in liver injury in up to 50% of patients receiving long-term treatment. The hepatotoxic effects of AMD are attributed to its disruption of lipid bilayers and interference with lysosomal and mitochondrial function. These alterations may result in microvesicular steatosis, hepatocellular ballooning, and Mallory body formation—ultimately culminating in hepatic fibrosis¹.

Amiodarone functions as a potent inhibitor of phospholipase A, leading to the accumulation of lipid-rich material within lysosomes. Another proposed mechanism underlying AMD-induced steatohepatitis involves the induction of endoplasmic reticulum (ER) stress. Studies indicate that repeated exposure to AMD triggers ER stress and augments lipolysis in adipose tissue, concurrently fostering a lipotoxic hepatic environment. These findings suggest that AMD-related liver injury arises from cumulative damage to both hepatic and adipose tissues².

Nicorandil is a well-established antianginal agent indicated for chronic stable angina. Multiple mechanisms contribute to the protective effects of nicorandil across various pathologies, mediated through either the opening of adenosine triphosphate-sensitive potassium (K_{ATP}) channels or nitric oxide (NO) donation³. The predominance of these mechanisms is influenced by the administered dose and the specific anatomical site of the pathology. In experimental models of myocardial and pulmonary fibrosis, renal injury, and glomerulonephritis, the protection afforded by nicorandil is mainly attributed to K_{ATP} channel opening; in contrast, NO donation predominates as the primary mechanism of protection in hepatic fibrosis and inflammatory bowel diseases⁴.

Mesenchymal stromal cells (MSCs) are multipotent cells sequestered in various tissues, including bone marrow, adipose tissue, umbilical cord, and dental pulp. The functional properties of MSCs, notably their differentiation capacity and immunoregulatory effects, diverge depending on the tissue

Cite this article : Mahmoud H, Harb I, El-hanbuli H, Rashwan E, Rashed LA, Ahmed AA, Mostafa A. Nicorandil and mesenchymal stromal cells attenuate amiodarone-induced liver fibrosis in experimental rats. *Biomed. Res. Ther.* 2026; 13(02):8223-8233.

source. MSCs have been extensively studied as a novel therapeutic for liver diseases due to their robust self-renewal potential, low inherent immunogenicity, and immunomodulatory profile⁵, in addition to their inherent capacity for migration and homing to damaged tissues⁶. In this study, we focused on bone marrow-derived MSCs (BM-MSCs) due to their well-established isolation and culture protocols, as well as their proven ability to promote tissue regeneration and modulate immune responses in liver injury models.

Given that amiodarone is frequently administered to elderly patients with comorbid cardiac disease, the development of effective prophylactic strategies to mitigate its hepatotoxic effects is imperative. This study aims to evaluate the hepatoprotective efficacy of nicorandil and mesenchymal stromal cells in ameliorating amiodarone-induced toxicity in a rat model.

MATERIAL - METHODS

Isolation and preparation of bone marrow-derived MSCs

The tibiae and femurs of six-week-old male albino rats were flushed with phosphate-buffered saline (PBS) to extract bone marrow. A density gradient (Ficoll-Paque, Pharmacia Ltd., Uppsala, Sweden) was employed to isolate mononuclear cells, which were subsequently resuspended in a culture medium comprising Dulbecco's Modified Eagle's Medium (DMEM, GIBCO/BRL), 10% fetal bovine serum (GIBCO/BRL), and 1% penicillin-streptomycin (GIBCO/BRL). Cells were incubated at 37°C in a 5% humidified atmosphere until reaching 80–90% confluence. Subsequently, cells were detached using 0.25% trypsin in 1 mM EDTA (GIBCO/BRL) and centrifuged at 2400 rpm for 20 minutes. BM-MSCs were cultured and expanded to passage 3 before being collected and stored at –80°C. Prior to administration, cell viability was assessed via trypan blue exclusion staining; only preparations with exceeding 95% viability were utilized⁷.

Experimental animals and ethical approval

This study (trial number: CU/III/F/16/21) was conducted using 36 male Sprague Dawley albino rats housed in the animal house unit following ethical approval from the Institutional Animal Care and Use Committee (CU/III/F/16/21). The study adhered to the ARRIVE guidelines. The sample size was determined using G-Power software, with liver function

improvement designated as the primary outcome. Based on Tao et al.⁸, an effect size of 0.66, an error of 0.05, and a statistical power of 80% were utilized for the calculation.

All animals were housed under standard laboratory conditions throughout the study. Rats were maintained in polypropylene cages with clean bedding under a controlled temperature of 22 ± 2°C, relative humidity of 50–60%, and a 12:12-hour light/dark cycle. Animals had *ad libitum* access to standard commercial chow and water. Health status and behavior were monitored daily.

Experimental design and grouping

After a one-week acclimatization period, rats were randomized into six study groups (n = 6 per group).

- Group 1 (Normal Control): Received PBS vehicle daily via oral gavage for 8 weeks.
- Group 2 (Nicorandil): Received nicorandil (10 mg/kg/day) dissolved in water via oral gavage for 8 weeks. This dose was selected based on its established protective effects in various rat models^{9–11}.
- Group 3 (BM-MSCs): Received cells/mL BM-MSCs suspended in 0.2 mL PBS intravenously via the tail vein at weeks 2, 4, and 6. This repeated administration schedule was designed to promote tissue repair and maximize engraftment⁷.
- Group 4 (Amiodarone): Received amiodarone (25 mg/kg/day) via oral gavage for 8 weeks. The dose was calculated according to dose conversion guidelines between animals and humans¹² and previous experimental models of organ toxicity^{13,14}.
- Group 5 (AMD + Nicorandil): Received amiodarone and nicorandil concurrently at the dosages and routes described above.
- Group 6 (AMD + MSCs): Received both amiodarone and MSCs at the dosages and schedules described above.

At the conclusion of the 8-week period, blood samples were collected from the retro-orbital venous plexus. Rats were subsequently anesthetized using urethane (0.7 mL/100 g, i.p.)¹³. All animals survived the treatment period without adverse effects. Euthanasia was performed via urethane overdose. Liver tissues were immediately preserved in PBS for biomolecular analysis and 10% neutral buffered formalin for histopathological examination.

Histological analysis

Liver samples were fixed in 10% buffered formalin for 24 hours. Paraffin sections (5 μ m thickness) were stained with hematoxylin and eosin (H&E) to assess pathological changes and Masson's Trichrome (MT) to evaluate the extent of fibrosis. Histopathological lesions—including microsteatosis, macrosteatosis, inflammatory infiltration, Kupffer cell hyperplasia, and sinusoidal dilatation—were graded on a numerical scale (0: minimal/none; 1: mild; 2: moderate; 3: severe) across six random fields per slide.

Biochemical and oxidative stress assays

Serum levels of ALT, AST, and albumin were quantified using commercial kits (Spectrum, Hannover, Germany) per the manufacturer's instructions. These enzymatic assays utilize substrate conversion (e.g., L-alanine or L-aspartate) to produce colored hydrazones, with absorbance measured at 520 nm.¹⁵

Serum malondialdehyde (MDA) and superoxide dismutase (SOD) levels were determined via ELISA (MyBioSource and LifeSpan BioSciences, respectively). Target quantitation was achieved using specific antibodies to capture the antigens, followed by enzymatic reaction-induced signaling proportional to the marker concentration¹⁶.

Quantitative Real-Time PCR (qRT-PCR)

Total RNA was extracted from homogenized liver tissue using the TRI reagent and Direct-zol™ RNA Miniprep Kit (ZYMO Research, USA). Reverse transcription and qRT-PCR were performed in a single step using the TransScript Green One-Step qRT-PCR SuperMix kit on a StepOne instrument (Applied Biosystems, USA). The thermal cycling profile included cDNA synthesis (45°C for 15 min), inactivation (95°C for 10 min), and 45 cycles of amplification (95°C for 10 s, 60°C for 30 s, and 72°C for 30 s). A melt-curve analysis was conducted to verify product specificity. Relative gene expression was calculated using the method, with GAPDH serving as the internal housekeeping gene.

Primer sequences:

- TGF- α : F: 5'-TGCTAATGGTGGACCGCAA-3', R: 5'-CACTGCTTCCCGAATGTCTGA-3'
- TNF- α : F: 5'-CCAGGAGAAAGTCAGCCTCCT-3', R: 5'-TCATACCAGGGCTTGAGCTCA-3'
- IL-6: F: 5'-GCCCTTCAGGAACAGCTATGA-3', R: 5'-TGTCACAACATCAGTCCCAAGA-3'
- GAPDH: F: 5'-CATGTTTCGTCATGGGGTGAACCA-3', R: 5'-AGTGATGGCATGGACTGTGGTCAT-3'

Statistical Analysis

Data were analyzed using SPSS (version 26) and are expressed as mean \pm standard deviation (SD). Comparisons between groups were performed via ANOVA followed by Tukey's post-hoc test. Histological injury scores were analyzed using the Kruskal-Wallis test followed by the Mann-Whitney U test, presented as median (interquartile range). Statistical significance was defined as $p < 0.05$.

RESULTS

MSCs isolation and identification

Cultured bone marrow-derived MSCs exhibited the characteristic fusiform, fibroblast-like morphology under phase contrast microscopy (Figure 1). Flow cytometric analysis confirmed the immunophenotype of MSCs, demonstrating positive expression of the mesenchymal surface markers CD105 (Figure 1) and CD90 (Figure 1), while showing negative expression for the hematopoietic marker CD34 (Figure 1). Cell viability prior to administration exceeded 95% as assessed by trypan blue exclusion.

Nicorandil and MSCs significantly improved liver function parameters

Amiodarone administration for eight weeks resulted in marked hepatic injury, as evidenced by significant elevations in serum liver enzymes compared to the control group. The amiodarone-treated group showed a greater than three-fold increase in ALT levels (62.17 ± 8.13 U/L) and approximately 2.5-fold increase in AST levels (56.50 ± 8.14 U/L) relative to controls (19.50 ± 5.79 U/L and 21.83 ± 2.79 U/L, respectively; $p < 0.001$). Concurrent treatment with either nicorandil or MSCs significantly attenuated these elevations. ALT levels decreased to 33.00 ± 4.2 U/L in the nicorandil-treated group and 31.00 ± 4.43 U/L in the MSC-treated group ($p < 0.001$ vs. amiodarone group). Similarly, AST levels were reduced to 28.67 ± 2.73 U/L and 32.67 ± 2.73 U/L following nicorandil and MSC treatment, respectively ($p < 0.001$ vs. amiodarone group). No significant differences in ALT or AST levels were observed between the nicorandil and MSC treatment groups ($p = 0.9$; Table 1). Serum albumin levels were significantly decreased in the amiodarone group (3.57 ± 0.39 g/dL) compared to controls (5.13 ± 0.64 g/dL; $p < 0.001$). Both treatment interventions significantly restored albumin levels, with values of 4.33 ± 0.27 g/dL in the nicorandil group ($p = 0.003$ vs. amiodarone) and 4.53 ± 0.25 g/dL in the MSC group ($p = 0.026$ vs.

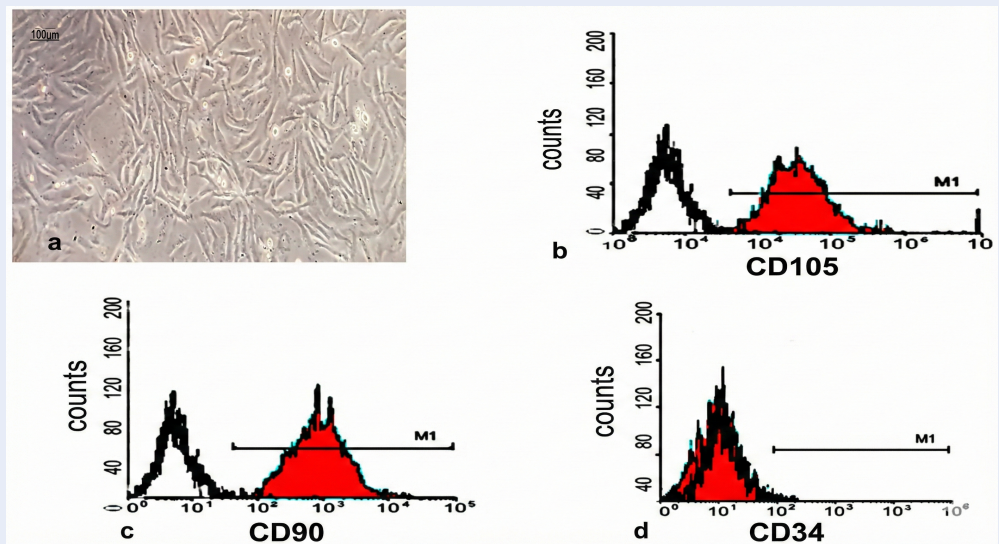


Figure 1: Characterization of bone marrow-derived mesenchymal stromal cells (BM-MSCs). (a) Phase-contrast photomicrograph showing cultured MSCs at passage 3 exhibiting characteristic fusiform, fibroblast-like morphology (scale bar = 100 μm). (b-d) Flow cytometric analysis of MSC surface markers demonstrating positive expression of (b) CD105 and (c) CD90, and (d) negative expression of the hematopoietic marker CD34.

amiodarone). Notably, albumin levels in the MSC-treated group approached control values. No significant difference in serum albumin was detected between the nicorandil and MSC groups ($p = 0.9$; Table 1). The control groups receiving nicorandil or MSCs alone showed no significant alterations in liver function parameters compared to the normal control group ($p > 0.05$).

Nicorandil and MSCs restored hepatic oxidative stress balance

Amiodarone administration induced significant oxidative stress, as demonstrated by a marked increase in serum MDA levels (40.80 ± 9.92 ng/mL) compared to controls (13.30 ± 1.29 ng/mL; $p < 0.001$), accompanied by a substantial reduction in SOD activity (2.89 ± 0.85 ng/mL vs. 7.76 ± 0.52 ng/mL in controls; $p < 0.001$). Treatment with either nicorandil or MSCs effectively reversed these alterations. MDA levels decreased significantly to 21.55 ± 2.64 ng/mL in the nicorandil group and 24.67 ± 4.77 ng/mL in the MSC group ($p < 0.001$ vs. amiodarone group). Concurrently, SOD levels increased to 6.46 ± 0.99 ng/mL and 6.52 ± 1.77 ng/mL following nicorandil and MSC treatment, respectively ($p < 0.001$ vs. amiodarone group). No significant differences in MDA or SOD levels were observed between the nicorandil and MSC treatment groups ($p = 0.8$ and $p = 0.9$, respectively). The nicorandil and MSC control groups ex-

hibited oxidative stress markers comparable to the normal control group ($p > 0.05$; Table 1).

Nicorandil and MSCs attenuated hepatic inflammation and fibrotic gene expression

Gene expression analysis revealed significant up-regulation of inflammatory and fibrotic mediators in the livers of amiodarone-treated rats. Relative to controls, the amiodarone group showed approximately 4.5-fold increase in IL-6 expression, 5-fold increase in TNF- α expression, and 4-fold increase in TGF- β expression ($p < 0.001$ for all; Figure 2).

Treatment with nicorandil significantly reduced the expression of all three markers. IL-6 expression decreased by approximately 60% compared to the amiodarone group, while TNF- α and TGF- β showed reductions of approximately 65% and 60%, respectively ($p < 0.001$). Similarly, MSC treatment resulted in significant downregulation of IL-6 (approximately 75% reduction), TNF- α (approximately 70% reduction), and TGF- β (approximately 65% reduction) relative to the amiodarone group ($p < 0.001$; Figure 2). Notably, a significant difference in IL-6 expression was observed between the treatment groups, with MSC-treated animals showing lower levels than nicorandil-treated animals ($p = 0.02$). However, no significant differences were detected between the nicorandil and MSC groups regarding TNF- α ($p = 0.1$) or TGF- β ($p = 0.8$) gene expression (Figure 2).

Table 1: Effect of nicorandil and MSCs on the liver enzymes (ALT, AST), albumin, and oxidative stress markers in the different studied groups

	Control (n=6)	NICO (10 mg/kg) (n=6)	MSCs (n=6)	AMIO (25 mg/kg) (n=6)	AMIO (25 mg/kg) + NICO (10 mg/kg) (n=6)	AMIO + MSCs (n=6)
ALT (U/L)	19.50±5.79	15.50±2.43	16.00±2.83	62.17±8.13*	33.00±4.2*#	31.00±4.43*#
AST (U/L)	21.83±2.79	22.33±3.88	21.67±4.63	56.50±8.14*	28.67±2.73#	32.67±2.73*#
Albumin (gm/dl)	5.13±0.64	5.28±0.31	5.32±0.40	3.57±0.39 *	4.33±0.27*#	4.53±0.25*#
MDA (ng/ml)	13.30±1.29	11.53±1.06	12.25±1.44	40.80±9.92*	21.55±2.64#	24.67±4.77*#
SOD (ng/ml)	7.76±0.52	9.02±0.67	8.43±1.09	2.89±0.85*	6.46±0.99#	6.52±1.77#

Abbreviations: AMIO: amiodarone, NICO: nicorandil, MSCs: mesenchymal stromal cells, ALT: Alanine transaminase, AST: Aspartate transaminase, NICO: Nicorandil, AMIO: Amiodarone, MSCs: Mesenchymal stromal cells, MDA: Malondialdehyde, SOD: Superoxide Dismutase; * significant difference versus the control group; # significant difference versus the amiodarone group

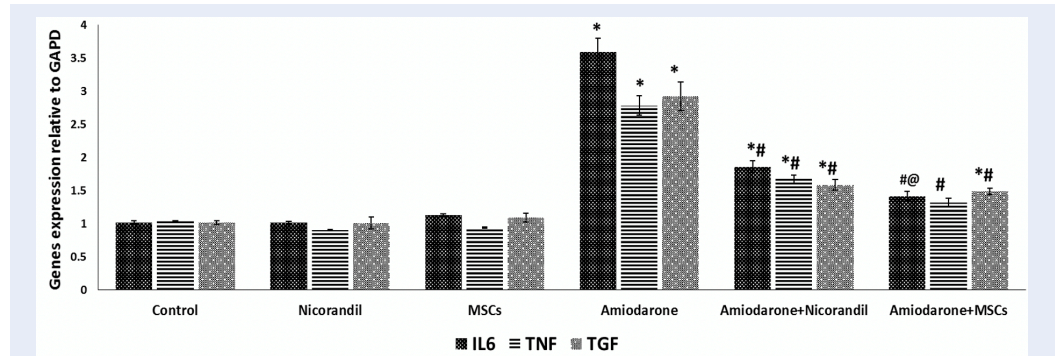


Figure 2: Effect of nicorandil and MSCs on hepatic inflammatory and fibrotic gene expression. Relative mRNA expression levels of (a) interleukin-6 (IL-6), (b) tumor necrosis factor-alpha (TNF-α), and (c) transforming growth factor-beta1 (TGF-β1) in liver tissues of the different study groups, normalized to GAPDH and expressed as fold change relative to the control group. Data are presented as mean ± SD (n=6 per group). *p < 0.05 versus control group; #p < 0.05 versus amiodarone group; @p < 0.05 versus nicorandil-treated group

Histopathological findings confirmed the hepatoprotective effects of nicorandil and MSCs

H&E staining

Histological examination of liver sections from the control, nicorandil-only, and MSC-only groups revealed preserved hepatic architecture with normal central veins, radially arranged cords of polygonal hepatocytes exhibiting acidophilic cytoplasm and large vesicular nuclei, occasional binucleation, and normal portal areas containing portal veins, hepatic arteries, and bile ducts (Figure 3).

In contrast, the amiodarone-treated group exhibited marked histopathological alterations, including central vein congestion, widespread microvesicular

and macrovesicular hepatic steatosis, nuclear pyknosis, prominent inflammatory cellular infiltration, and periportal Kupffer cell hyperplasia (Figure 3). The median liver injury score was significantly elevated in the amiodarone group compared to controls (p < 0.001; Figure 3).

Treatment with nicorandil markedly ameliorated these changes, with liver sections showing preserved hepatic structure, only slight central and portal vein congestion, and mild Kupffer cell hypertrophy (Figure 3). The liver injury score was significantly reduced compared to the amiodarone group (p < 0.001; Figure 3).

The MSC-treated group demonstrated substantial improvement in liver architecture, with intact central and portal areas and only minimal periportal

Kupffer cell hyperplasia (Figure 3). The liver injury score was significantly lower than both the amiodarone group ($p < 0.001$) and the nicorandil-treated group ($p < 0.05$; Figure 3).

Masson's trichrome staining

Masson's trichrome staining revealed minimal perivascular and periportal collagen deposition in the control, nicorandil-only, and MSC-only groups, consistent with normal hepatic architecture (Figure 4). The amiodarone-treated group exhibited extensive fibrosis, characterized by dense collagen bundles surrounding dilated central veins and within portal areas, accompanied by dilated proliferating bile ducts and congested hepatic arteries. Quantitative analysis confirmed a significant increase in the area percentage of collagen deposition in the amiodarone group compared to controls ($p < 0.001$; Figure 4).

Nicorandil treatment significantly reduced collagen deposition, with only minimal collagen fibers observed in central and periportal regions ($p < 0.001$ vs. amiodarone group; Fig. 4a-b). Similarly, MSC treatment attenuated hepatic fibrosis, showing moderate collagen deposition around central veins and portal structures, with a significant reduction in the fibrotic area compared to the amiodarone group ($p < 0.001$; Figure 4).

DISCUSSION

The present study demonstrates, for the first time, the comparative hepatoprotective effects of nicorandil and bone marrow-derived mesenchymal stromal cells (BM-MSCs) against amiodarone-induced liver fibrosis in rats. Our findings reveal that both interventions effectively attenuated hepatic injury through complementary mechanisms involving antioxidant defense, anti-inflammatory action, and antifibrotic activity, with MSCs showing superior efficacy in reducing hepatic inflammation and histological injury.

Amiodarone-induced hepatotoxicity represents a significant clinical challenge, particularly in elderly patients requiring long-term antiarrhythmic therapy¹⁷. The pathogenesis involves mitochondrial dysfunction, phospholipidosis, and oxidative stress, ultimately progressing from steatosis to irreversible cirrhosis^{18,19}. In our experimental model, eight weeks of amiodarone administration produced classic features of hepatic injury, including elevated transaminases, hypoalbuminemia, oxidative stress, and marked fibrotic changes—consistent with previous reports^{1,20}.

The significant elevation of ALT and AST observed in amiodarone-treated rats reflects hepatocellular membrane disruption and enzyme leakage²⁰, while the concomitant reduction in serum albumin indicates impaired synthetic function secondary to hepatocyte degeneration¹. Both nicorandil and MSCs effectively reversed these abnormalities, with MSCs restoring albumin to near-normal levels. This functional improvement was accompanied by restoration of the oxidant/antioxidant balance, as evidenced by reduced MDA and increased SOD activity.

The antioxidant properties of nicorandil likely involve dual mechanisms: direct hydroxyl radical scavenging via its nicotinamide moiety²¹ and indirect effects through mitochondrial K ATP channel opening, which reduces mitochondrial membrane potential and subsequent ROS generation²². These findings align with previous studies demonstrating nicorandil's ability to attenuate hepatic oxidative stress in various injury models²³⁻²⁵. Similarly, MSCs exert antioxidant effects through both direct free radical scavenging and indirect upregulation of endogenous antioxidant defenses, including GSH and SOD^{26,27}. The comparable antioxidant efficacy of both interventions suggests that oxidative stress represents a central, targetable pathway in amiodarone-induced hepatotoxicity.

The marked upregulation of pro-inflammatory cytokines (IL-6 and TNF- α) in amiodarone-treated rats implicates inflammatory signaling in the pathogenesis of AMD-induced liver injury. Both nicorandil and MSCs significantly suppressed these mediators, consistent with their established immunomodulatory properties^{24,25,28}. Notably, MSCs demonstrated superior IL-6 suppression compared to nicorandil, suggesting enhanced anti-inflammatory efficacy that may reflect the complex paracrine signaling networks employed by MSCs, including secretion of TSG-6, PGE2, and other immunomodulatory factors^{28,29}.

Hepatic fibrosis represents the culmination of chronic injury and inflammation, driven primarily by TGF- β -mediated activation of hepatic stellate cells and excessive ECM deposition³⁰. The substantial reduction in TGF- β expression following both interventions correlated with marked histological improvement, including reduced collagen deposition on Masson's trichrome staining and lower injury scores on H&E examination.

Nicorandil's antifibrotic effects have been previously documented in bile duct ligation models, where treatment downregulated α -SMA expression

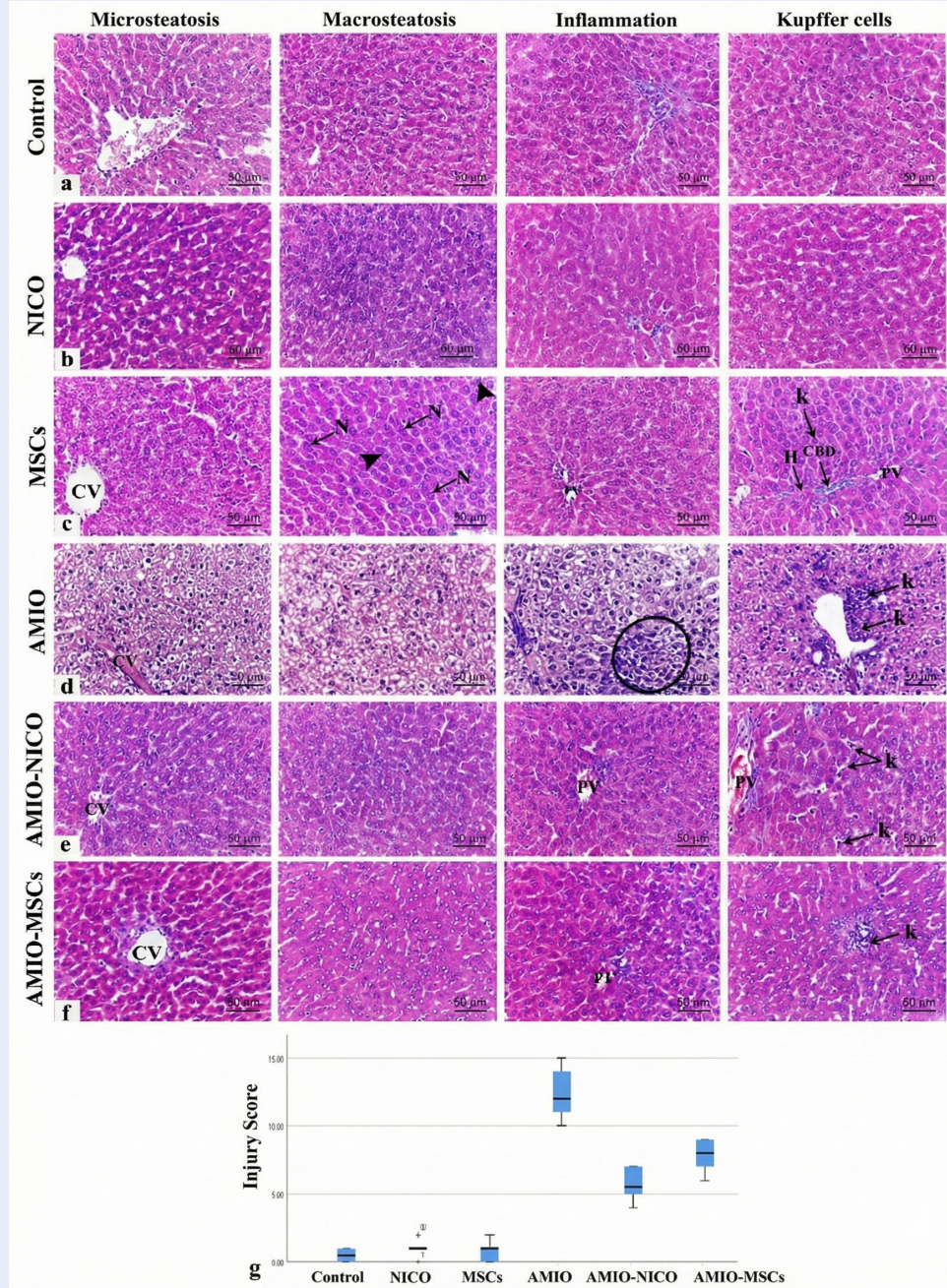


Figure 3: Representative photomicrographs of hematoxylin and eosin (H&E)-stained liver sections (scale bar = 50 μm) and quantitative histological injury scores. (a) Control group showing normal hepatic architecture with central vein (CV), cords of hepatocytes with acidophilic cytoplasm and vesicular nuclei (N), occasional binucleation (arrowheads), sinusoids lined by Kupffer cells (k), and normal portal area containing portal vein (PV), hepatic artery (H), and bile duct (CBD). **(b)** Nicorandil-only group and **(c)** MSC-only group showing preserved hepatic structure comparable to controls. **(d)** Amiodarone-treated group exhibiting central vein congestion, widespread microvesicular and macrovesicular steatosis, nuclear pyknosis, inflammatory infiltration (circle), and periportal Kupffer cell hyperplasia (k). **(e)** Amiodarone + nicorandil group showing preserved hepatic architecture with mild central/portal congestion and mild Kupffer cell hypertrophy (k). **(f)** Amiodarone + MSCs group demonstrating improved liver architecture with intact central and portal areas and minimal periportal Kupffer cell hyperplasia. **(g)** Liver injury scores presented as median with interquartile range (n=6). *p < 0.05 versus control groups; #p < 0.05 versus amiodarone group; @p < 0.05 versus nicorandil-treated group.

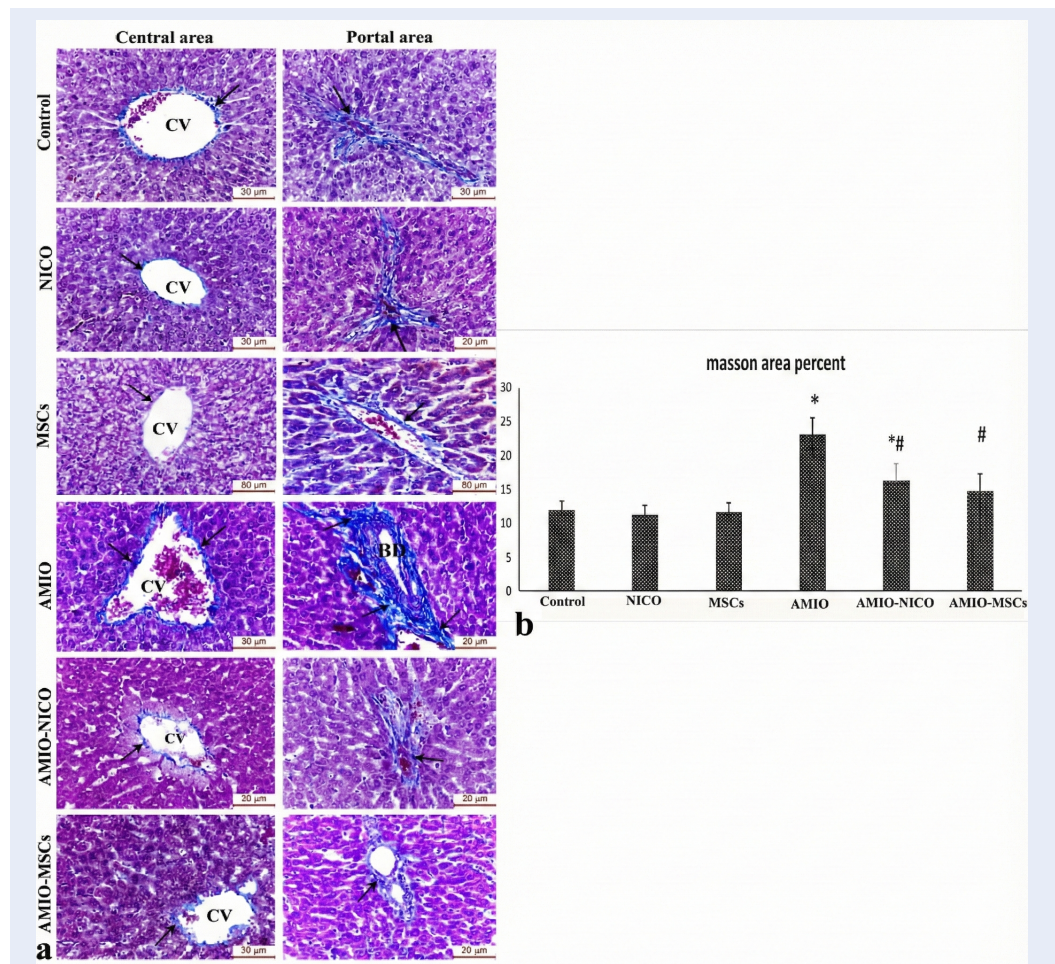


Figure 4: Assessment of hepatic collagen deposition by Masson's trichrome staining. (a) Representative photomicrographs of liver sections stained with Masson's trichrome (scale bar = 50 μm). Control, nicorandil-only, and MSC-only groups show thin uniform collagen fibers around central veins and portal areas. The amiodarone-treated group reveals dense collagen bundles around a dilated central vein and portal area, with dilated proliferating bile duct (BD) and congested hepatic artery (A). The amiodarone + nicorandil group shows minimal collagen deposition in central and periportal regions. The amiodarone + MSCs group demonstrates moderate collagen deposition around central veins, bile ducts, and portal veins. Arrows indicate collagen deposits. (b) Quantitative analysis of the area percentage of collagen deposition. Data are presented as mean ± SD (n=6). *p < 0.05 versus control group; #p < 0.05 versus amiodarone group.

and improved hepatic architecture^{30,31}. These effects are attributed to K ATP channel opening and NO donation, which collectively suppress stellate cell activation and promote vasodilation, improving hepatic microcirculation. Our findings extend these observations to a clinically relevant model of drug-induced fibrosis.

MSCs modulate fibrosis through multiple mechanisms, including differentiation into hepatocyte-like cells, direct inhibition of hepatic stellate cell activation, and paracrine-mediated modulation of the TGF-β/SMAD signaling pathway^{14,29,32,33}. The superior histological improvement observed with

MSCs—particularly the reduction in Kupffer cell hyperplasia and inflammatory infiltration—likely reflects their capacity for sustained immunomodulation and tissue integration.

While both interventions demonstrated significant hepatoprotection, subtle differences emerged. MSCs showed enhanced efficacy in reducing IL-6 expression and histological injury scores, suggesting that cell-based therapy may offer advantages for severe inflammatory injury. However, nicorandil—an orally administered, well-tolerated drug with established cardiovascular indications—presents a more immediately accessible prophylactic strategy for pa-

tients requiring amiodarone therapy. The comparable effects on liver enzymes, oxidative stress markers, and TGF- β expression suggest that nicorandil could serve as a practical adjunctive therapy, while MSCs may be reserved for cases of established or progressive fibrosis.

This study has several limitations. First, the prophylactic administration protocol (concurrent treatment with amiodarone) does not address the therapeutic efficacy of these interventions in established liver fibrosis. Future studies should investigate treatment following fibrosis development to assess regenerative potential. Second, while we demonstrate antioxidant, anti-inflammatory, and antifibrotic effects, the precise molecular mechanisms—particularly regarding differential signaling pathway activation (e.g., PI3K/AKT, Nrf2, autophagy)—require further elucidation through targeted inhibitors or knockout models. Third, variability in MSC sources and isolation protocols may influence therapeutic efficacy and limit generalizability. Fourth, the sample size, while statistically justified, was relatively small, and assessments were not performed blinded to group allocation, introducing potential bias. Finally, as a preclinical model, these findings require validation in human studies, although the translational relevance is supported by the use of clinically relevant doses and administration routes.

CONCLUSION

Nicorandil and BM-MSCs effectively attenuate amiodarone-induced liver fibrosis in rats through coordinated antioxidant, anti-inflammatory, and antifibrotic mechanisms. Both interventions normalized liver function tests, restored oxidative balance, suppressed pro-inflammatory and profibrotic mediators, and improved histological architecture. These findings support further investigation of nicorandil as an accessible prophylactic strategy and MSCs as a potential therapeutic option for amiodarone-induced hepatotoxicity, with the goal of improving the safety profile of this essential antiarrhythmic medication.

ABBREVIATIONS

ALT: Alanine transaminase; **AMD:** Amiodarone; **AST:** Aspartate transaminase; **BM-MSCs:** Bone marrow-derived mesenchymal stromal cells; **DMEM:** Dulbecco's Modified Eagle's Medium; **EDTA:** Ethylenediaminetetraacetic acid; **ELISA:** Enzyme-linked immunosorbent assay; **ER:** Endoplasmic reticulum; **GAPDH:**

Glyceraldehyde-3-phosphate dehydrogenase; **H&E:** Hematoxylin and eosin; **IL-6:** Interleukin-6; **K⁺ ATP :** Adenosine triphosphate-sensitive potassium; **MDA:** Malondialdehyde; **MSCs:** Mesenchymal stromal cells; **MT:** Masson's Trichrome; **NICO:** Nicorandil; **NO:** Nitric oxide; **PBS:** Phosphate-buffered saline; **qPCR:** Quantitative polymerase chain reaction; **qRT-PCR:** Quantitative real-time polymerase chain reaction; **SOD:** Superoxide dismutase; **TGF- β 1:** Transforming growth factor beta-1; **TNF- α :** Tumor necrosis factor alpha

ACKNOWLEDGMENTS

None.

AUTHOR'S CONTRIBUTIONS

Author's contribution: The concept of the study was constructed by Heba Mahmoud and Inas A Harb. The experiments were conducted by Heba Mahmoud, Inas A Harb, Eman Rashwan, and Abeer Mostafa. Biochemical studies were done by Laila A Rashed, Abeer Mostafa and Azza Abusree. Hala El-hanbuli performed the histopathological examination. Statistical analysis was performed by Abeer Mostafa and Eman Rashwan. Writing the first draft was performed by Abeer Mostafa. The revision and editing were done by Azza Abusree. The manuscript was revised and approved by all the contributing authors. All authors read and approved the final manuscript.

FUNDING

None.

AVAILABILITY OF DATA AND MATERIALS

Data and materials used and/or analyzed during the current study are available from the corresponding author on reasonable request.

ETHICS APPROVAL AND CONSENT TO PARTICIPATE

This study was performed in line with the principles of the Declaration of Helsinki. Approval was granted by the Institutional Animal Care and Use of Laboratory Animals (CU/III/F/16/21).

CONSENT FOR PUBLICATION

Not applicable.

DECLARATION OF GENERATIVE AI AND AI-ASSISTED TECHNOLOGIES IN THE WRITING PROCESS

The authors declare that they have not used generative AI (a type of artificial intelligence technology that can produce various types of content including text, imagery, audio and synthetic data. Examples include ChatGPT, NovelAI, Jasper AI, Rytr AI, DALL-E, etc) and AI-assisted technologies in the writing process before submission.

COMPETING INTERESTS

The authors declare that they have no competing interests.

REFERENCES

1. LiverTox: Clinical and Research Information on Drug-Induced Liver Injury. Bethesda (MD): National Institute of Diabetes and Digestive and Kidney Diseases; 2012. [Internet]. PMID: 31643176.
2. Hubel E, Fishman S, Holopainen M, Käkälä R, Shaffer O, Hourli I, et al. Repetitive amiodarone administration causes liver damage via adipose tissue ER stress-dependent lipolysis, leading to hepatotoxic free fatty acid accumulation. *American Journal of Physiology-Gastrointestinal and Liver Physiology*. 2021;321(3):G298–G307.
3. Harb IA, Ashour H, Sabry D, El-Yasergy DF, Hamza WM, Mostafa A. Nicorandil prevents the nephrotoxic effect of cyclosporine-A in albino rats through modulation of HIF-1 α /VEGF/eNOS signaling. *Canadian Journal of Physiology and Pharmacology*. 2021 Apr;99(4):411–417. PMID: 32822562. Available from: [10.1139/cjpp-2020-0012](https://doi.org/10.1139/cjpp-2020-0012).
4. Ahmed LA. Nicorandil: A drug with ongoing benefits and different mechanisms in various diseased conditions. *Indian Journal of Pharmacology*. 2019;51(5):296–301. PMID: 31831918. Available from: [10.4103/ijp.IJP_298_19](https://doi.org/10.4103/ijp.IJP_298_19).
5. Liu WH, Song FQ, Ren LN, Guo WQ, Wang T, Feng YX, et al. The multiple functional roles of mesenchymal stem cells in participating in treating liver diseases. *Journal of Cellular and Molecular Medicine*. 2015 Mar;19(3):511–520. PMID: 25534251. Available from: [10.1111/jcmm.12482](https://doi.org/10.1111/jcmm.12482).
6. Karp JM, Teo GSL. Mesenchymal stem cell homing: the devil is in the details. *Cell Stem Cell*. 2009 Mar;4(3):206–216. PMID: 19265660. Available from: [10.1016/j.stem.2009.02.001](https://doi.org/10.1016/j.stem.2009.02.001).
7. Farouk S, Sabet S, Abu Zahra FA, El-Ghor AA. Bone marrow derived-mesenchymal stem cells downregulate IL17A dependent IL6/STAT3 signaling pathway in CCl4-induced rat liver fibrosis. *PLOS ONE*. 2018 Oct;13(10):e0206130. PMID: 30346985. Available from: [10.1371/journal.pone.0206130](https://doi.org/10.1371/journal.pone.0206130).
8. Wu T, Li J, Li Y, Song H. Antioxidant and Hepatoprotective Effect of Swertiamarin on Carbon Tetrachloride-Induced Hepatotoxicity via the Nrf2/HO-1 Pathway. *Cell Physiology and Biochemistry*. 2017;41(6):2242–2254. PMID: 28448964. Available from: [10.1159/000475639](https://doi.org/10.1159/000475639).
9. Aizawa K, Takahari Y, Higashijima N, Serizawa K, Yogo K, Ishizuka N, et al. Nicorandil prevents sirolimus-induced production of reactive oxygen species, endothelial dysfunction, and thrombus formation. *Journal of Pharmacological Sciences*. 2015 Mar;127(3):284–291. PMID: 25837924. Available from: [10.1016/j.jphs.2014.12.017](https://doi.org/10.1016/j.jphs.2014.12.017).
10. Saito M, Ohmasa F, Tsounapi P, Inoue S, Dimitriadis F, Kinoshita Y, et al. Nicorandil ameliorates hypertension-related bladder dysfunction in the rat. *Neurourology and Urodynamics*. 2012 Jun;31(5):695–701. PMID: 22473863. Available from: [10.1002/nau.21213](https://doi.org/10.1002/nau.21213).
11. Shimizu S, Saito M, Kinoshita Y, Ohmasa F, Dimitriadis F, Shomori K, et al. Nicorandil ameliorates ischaemia-reperfusion injury in the rat kidney. *British Journal of Pharmacology*. 2011 May;163(2):272–282. PMID: 21250976. Available from: [10.1111/j.1476-5381.2011.01231.x](https://doi.org/10.1111/j.1476-5381.2011.01231.x).
12. Nair AB, Jacob S. A simple practice guide for dose conversion between animals and human. *Journal of Basic and Clinical Pharmacology*. 2016 Mar;7(2):27–31. PMID: 27057123. Available from: [10.4103/0976-0105.177703](https://doi.org/10.4103/0976-0105.177703).
13. Harb I, Ashour H, Rashed LA, Mostafa A, Samir M, Aboulhoda BE, et al. Nicorandil mitigates amiodarone-induced pulmonary toxicity and fibrosis in association with the inhibition of lung TGF- β 1/PI3K/Akt1-p/mTOR axis in rats. *Clinical and Experimental Pharmacology and Physiology*. 2023 Jan;50(1):96–106. PMID: 36208078. Available from: [10.1111/1440-1681.13728](https://doi.org/10.1111/1440-1681.13728).
14. Ghabrial MMM, Salem MFM, El Ela AAMA, El Deeb SAA. The possible therapeutic role of mesenchymal stem cells in amiodarone-induced lung injury in adult male albino rats. *Tanta Medical Journal*. 2018 Jul-Sep;46(3):172–182. Available from: [10.4103/tmj.tmj_4_18](https://doi.org/10.4103/tmj.tmj_4_18).
15. Sahoo D, Rukmini M, Ray R. Quantitative analysis of serum level alanine and aspartate aminotransferases, γ -Glutamyl transferase and alkaline phosphatase as predictor of liver diseases. *American International Journal of Research in Formal, Applied & Natural Sciences*. 2015;9(1):51–55.
16. Yener MD, Çolak T, Özsoy ÖD, Eraldemir FC. Alterations in catalase, superoxide dismutase, glutathione peroxidase and malondialdehyde levels in serum and liver tissue under stress conditions. *Istanbul Tip Fakültesi Dergisi*. 2024;87(2):145–152.
17. Nasser M, Larsen TR, Waanbah B, Sidiqi I, McCullough PA. Hyperacute drug-induced hepatitis with intravenous amiodarone: case report and review of the literature. *Drug Health-care and Patient Safety*. 2013 Sep;5:191–198. PMID: 24109195. Available from: [10.2147/DHPS.S48640](https://doi.org/10.2147/DHPS.S48640).
18. Begriche K, Massart J, Robin MA, Borgne-Sanchez A, Fromenty B. Drug-induced toxicity on mitochondria and lipid metabolism: Mechanistic diversity and deleterious consequences for the liver. *Journal of Hepatology*. 2011;54(4):773–794. Available from: [10.1016/j.jhep.2010.11.006](https://doi.org/10.1016/j.jhep.2010.11.006).
19. Lewis JH, Mullick F, Ishak KG, Ranard RC, Ragsdale B, Perse RM, et al. Histopathologic analysis of suspected amiodarone hepatotoxicity. *Human Pathology*. 1990 Jan;21(1):59–67. PMID: 2403975. Available from: [10.1016/0046-8177\(90\)90076-H](https://doi.org/10.1016/0046-8177(90)90076-H).
20. Serviddio G, Bellanti F, Giudetti AM, Gnani GV, Capitanio N, Tamborra R, et al. Mitochondrial oxidative stress and respiratory chain dysfunction account for liver toxicity during amiodarone but not dronedarone administration. *Free Radical Biology and Medicine*. 2011 Dec;51(12):2234–2242. PMID: 21971348. Available from: [10.1016/j.freeradbiomed.2011.09.004](https://doi.org/10.1016/j.freeradbiomed.2011.09.004).
21. Wincewicz A, Woltanowski P. Leopold Auerbach's achievements in the field of vascular system. *Angiogenesis*. 2020 Nov;23(4):577–579. PMID: 32719962. Available from: [10.1007/s10456-020-09739-5](https://doi.org/10.1007/s10456-020-09739-5).
22. Lu C, Minatoguchi S, Arai M, Wang N, Chen XH, Bao N, et al. Nicorandil improves post-ischemic myocardial dysfunction in association with opening the mitochondrial K(ATP) channels and decreasing hydroxyl radicals in isolated rat hearts. *Circulation Journal*. 2006 Dec;70(12):1650–1654. PMID: 17127815. Available from: [10.1253/circj.70.1650](https://doi.org/10.1253/circj.70.1650).
23. Abdel-Sattar AR, Abo-Saif AA, Aboyoussif AM. Nicorandil and atorvastatin attenuate carbon tetrachloride-induced liver fibrosis in rats. *Immunopharmacology and Immunotoxicology*. 2020 Dec;42(6):582–593. PMID: 32988255. Available from: [10.1080/08923973.2020.1830104](https://doi.org/10.1080/08923973.2020.1830104).
24. Elshazly SM. Ameliorative effect of nicorandil on high fat diet induced non-alcoholic fatty liver disease in rats. *European Journal of Pharmacology*. 2015 Feb;748:123–132. PMID: 25542756. Available from: [10.1016/j.ejphar.2014.12.017](https://doi.org/10.1016/j.ejphar.2014.12.017).
25. El-Kashef DH. Nicorandil ameliorates pulmonary inflammation and fibrosis in a rat model of silicosis. *International Im-*

- munopharmacology. 2018 Nov;64:289–297. PMID: 30223191. Available from: [10.1016/j.intimp.2018.09.017](https://doi.org/10.1016/j.intimp.2018.09.017).
26. Fan XL, Zhang Y, Li X, Fu QL. Mechanisms underlying the protective effects of mesenchymal stem cell-based therapy. *Cellular and Molecular Life Sciences*. 2020;77(14):2771–2794.
 27. Costa Gonçalves F, Grings M, Nunes NS, Pinto FO, Garcez TN, Visioli F, et al. Antioxidant properties of mesenchymal stem cells against oxidative stress in a murine model of colitis. *Biotechnology Letters*. 2017 Apr;39(4):613–622. PMID: 28032203. Available from: [10.1007/s10529-016-2272-3](https://doi.org/10.1007/s10529-016-2272-3).
 28. Wan YM, Li ZQ, Zhou Q, Liu C, Wang MJ, Wu HX, et al. Mesenchymal stem cells alleviate liver injury induced by chronic-binge ethanol feeding in mice via release of TSG6 and suppression of STAT3 activation. *Stem Cell Research & Therapy*. 2020 Jan;11(1):24. PMID: 31931878. Available from: [10.1186/s13287-019-1547-8](https://doi.org/10.1186/s13287-019-1547-8).
 29. Lee C, Kim M, Han J, Yoon M, Jung Y. Mesenchymal Stem Cells Influence Activation of Hepatic Stellate Cells, and Constitute a Promising Therapy for Liver Fibrosis. *Biomedicines*. 2021 Nov;9(11):1598. PMID: 34829827. Available from: [10.3390/biomedicines9111598](https://doi.org/10.3390/biomedicines9111598).
 30. Mohamed YS, Ahmed LA, Salem HA, Agha AM. Role of nitric oxide and KATP channel in the protective effect mediated by nicorandil in bile duct ligation-induced liver fibrosis in rats. *Biochemical Pharmacology*. 2018 May;151:135–142. PMID: 29522711. Available from: [10.1016/j.bcp.2018.03.003](https://doi.org/10.1016/j.bcp.2018.03.003).
 31. Ishibashi H, Nakamura M, Komori A, Migita K, Shimoda S. Liver architecture, cell function, and disease. *Seminars in Immunopathology*. 2009 Sep;31(3):399–409. PMID: 19468732. Available from: [10.1007/s00281-009-0155-6](https://doi.org/10.1007/s00281-009-0155-6).
 32. Xie G, Diehl AM. Evidence for and against epithelial-to-mesenchymal transition in the liver. *American Journal of Physiology-Gastrointestinal and Liver Physiology*. 2013 Dec;305(12):G881–G890. PMID: 24157970. Available from: [10.1152/ajpgi.00289.2013](https://doi.org/10.1152/ajpgi.00289.2013).
 33. Zhang L, Zhou D, Li J, et al. Effects of Bone Marrow-Derived Mesenchymal Stem Cells on Hypoxia and the Transforming Growth Factor β 1 (TGF β -1) and SMADs Pathway in a Mouse Model of Cirrhosis. *Medical Science Monitor*. 2019;p. 7182–7190. Available from: [10.12659/MSM.91642](https://doi.org/10.12659/MSM.91642).
 34. Kasama S, Toyama T, Iwasaki T, Sumino H, Kumakura H, Minami K, et al. Effects of oral nicorandil therapy on sympathetic nerve activity and cardiac events in patients with chronic heart failure: subanalysis of our previous report using propensity score matching. *European Journal of Nuclear Medicine and Molecular Imaging*. 2014 Jan;41(1):144–154. PMID: 23982455. Available from: [10.1007/s00259-013-2538-0](https://doi.org/10.1007/s00259-013-2538-0).
 35. Kang SH, Kim MY, Eom YW, Baik SK. Mesenchymal Stem Cells for the Treatment of Liver Disease: Present and Perspectives. *Gut and Liver*. 2020 May;14(3):306–315. PMID: 31581387. Available from: [10.5009/gnl18412](https://doi.org/10.5009/gnl18412).
 36. Altaib Z, Sabbah WS, Rashwan EK, Albrakati A, Mostafa A. Bone Marrow-derived Mesenchymal Stem Cells Reverse Hepatic Fibrosis, Improved Vascularity, and Attenuate the Apoptosis in Carbon Tetrachloride-induced Hepatic Fibrosis Experimental Rats. *Open Access Macedonian Journal of Medical Sciences*. 2021 Aug;9(A):698–706.
 37. Durukan AB, Erdem B, Durukan E, Sevim H, Karaduman T, Gurbuz HA, et al. May toxicity of amiodarone be prevented by antioxidants? A cell-culture study. *Journal of Cardiothoracic Surgery*. 2012 Jun;7(1):61. PMID: 22741616. Available from: [10.1186/1749-8090-7-61](https://doi.org/10.1186/1749-8090-7-61).